Seismic viscoelastic attenuation

Submitted to:

Encyclopedia of Solid Earth Geophysics
Harsh Gupta (ed.)
Springer

Prof. Vernon F. Cormier
Physics Department
University of Connecticut
Storrs, CT 06269-3046 USA
E-mail: vernon.cormier@uconn.edu
Tel: 860-486-3547
Fax: 860-486-3346

SEISMIC VISCOELASTIC ATTENUATION

Synonyms

Seismic intrinsic attenuation

Definitions

Linear viscoelastic attenuation. The loss of energy to heat within a material as an elastic wave propagates through the material, in which the resultant elastic deformation (strain) in the material lags in time the applied stress induced by the wave.

Apparent seismic Q. A factor defining an exponential decrease with frequency f and propagation time T of a seismic body wave given by the expression $\exp(-\pi f T/Q)$. The apparent Q combines the energy lost to heat and with the energy lost to elastic scattering.

Introduction

The amplitude of seismic waves decreases with increasing distance from earthquake, explosion, and impact sources. How this amplitude decrease, occurs, how rapidly it occurs, and how it depends on frequency of the seismic waves is fundamentally important to the efforts to describe Earth structure and seismic sources.

Seismic attenuation and its variation with location within the Earth are useful for determining the type and state of the rocks and minerals composing the Earth. In addition to providing information on a physical property, research in seismic attenuation has also been strongly motivated by more practical problems. One problem has been the prediction of ground motion due to probable earthquakes in different regions. The frequency content and decay with distance of this strong ground motion is an important input to the design of earthquake resistant structures and to disaster forecasting (see *Earthquake strong ground motion forecast*). Another problem has been to estimate the size and detectability of underground nuclear tests (see *Seismic monitoring of nuclear explosions*).

How do seismic waves attenuate?

The attenuation of seismic waves is due to three effects: geometric spreading, intrinsic attenuation, and scattering.

Geometric spreading

Geometric spreading is simply the energy density decrease that occurs as an elastic wavefront expands. In a homogeneous Earth of constant velocity and density, the geometric spreading of a seismic body waves is proportional to the reciprocal of the distance between source and receiver. In the real Earth, velocity and density vary strongly with depth and less so laterally. Given a model of this variation, however, the geometric spreading of a body wave can be easily calculated (see *Seismic, ray theory*).

Intrinsic attenuation

Intrinsic (viscoelastic) attenuation is energy lost to heat and internal friction during the passage of an elastic wave. The microscopic mechanisms of intrinsic attenuation have been described in several different ways, including the resistive and viscous properties of oscillator models of the atoms in crystalline lattices, the movement of interstitial fluids between grain boundaries and cracks, and the frictional sliding of cracks. Jackson (1993 and 2007) reviews laboratory experiments that investigate microscopic mechanisms of intrinsic attenuation. This article concentrates on the measurement of intrinsic attenuation from recordings of seismic waves at great distance.

Scattering attenuation

Scattering attenuation is not energy loss to heat or random motions on the scale of atoms, but rather elastic energy that is scattered and redistributed into directions away from the receiver or into waves arriving in later time windows at the receiver (see *Seismic, scattering*). Scattering takes place by reflection, refraction, and conversion of elastic energy by wavelength-scale irregularities in the medium. These irregularities are discontinuous or rapid variations in the velocity and/or density of the medium. In the crust and uppermost mantle, variations in velocity and density can be particularly strong in the lateral as well as the vertical direction.

Linear Viscoelasticity

Rheology

A stress is a vector force per unit area applied to a solid. A strain is non-dimensional measure of the deformation of the solid due to the applied stress, such as the change in a length element divided by the original length. The equation that relates stress and strain is sometimes termed the *rheology* or the *constitutive* relation (see *Mantle rheology*). A linear viscoelastic rheology can be described by a linear differential equation:

$$L_1 \sigma(t) = L_2 \varepsilon(t) \qquad (1)$$

Where L_1 and L_2 are any linear combinations of operators of the time $\frac{d^n}{dt^n}$ or $\int dt^n$. This type of equation can describe both the elastic strain of a material over a short time interval of applied stress as well as its viscous behavior and flow over a longer time interval (Gross ,1953; Nowick and Berry, 1972; Jackson et al. 2005).

Anelastic hysteresis

Seismic oscillations at distances beyond several fault lengths from an earthquake excite small strains less than 10^{-6}. These strains are recoverable during a cycle of seismic oscillation and lag the applied stress of the oscillation in time. Because of the time lag, a cycle of increasing and decreasing stress does not produce a perfectly proportional increase and decrease in strain. Instead a hysteresis loop occurs (Figure 1). The area enclosed by the hysteresis curve is a measure of the energy lost to heat and internal friction. During the stress cycle associated with the passage of a seismic wave, the energy lost to this internal friction is not available to deform the adjacent regions of the solid ahead of the wavefront and the amplitude of the wave decreases.

From the hysteresis curve, one can see that the stress-strain relation cannot be described by a simple constant of proportionality in the time domain. A more complicated relation involving an integral over time is required to describe strain at any instant of time as a function of the prior time history of the applied stress. By Fourier transforming the rheologic equation, however, and keeping only terms describing the short-term anelastic behavior, the stress-strain relation can be simply expressed by means of either a complex elastic modulus $\widehat{G}(\omega)$ or by its reciprocal, the complex elastic compliance, $\widehat{J}(\omega)$:

$$\widehat{\sigma}(\omega)=\widehat{G}(\omega)\,\varepsilon(\omega) \qquad (2a)$$

$$\widehat{\varepsilon}(\omega)=\widehat{J}(\omega)\,\widehat{\sigma}(\omega) \qquad (2b)$$

The elastic modulus $\widehat{G}$ and compliance $\widehat{J}$ must be a complex numbers to describe the phase lag of strain. $\widehat{G}$ and $\widehat{J}$ must also be frequency dependent because the phase lag of strain depends on the time history of stress, the shape of the hysteresis curve changing with different load histories. The trend of the frequency dependence can be inferred from the time lag of strain.

A feature of the complex modulus is that its real part will be smaller at zero or very low frequency and larger at infinite or very high frequency. That is, there will be an instantaneous response of strain to the applied stress, which is smaller than the eventual equilibrium response after longer time. The difference between the modulus at infinite frequency $G(\infty)$, representing the instantaneous or *unrelaxed* response, and the low frequency limit of the modulus $G(0)$, for the equilibrium or *relaxed* response, is called the *modulus defec*t ΔG, with

$$\Delta G = G(\infty) - G(0) \qquad (3)$$

The relaxed and unrelaxed moduli are pure real numbers that can be determined by observing a sequence of hysteresis curves for increasing frequencies of monochromatic loads. The frequency dependence of the real part of the modulus of at frequencies between 0 and ∞ implies that the propagation of a stress pulse will be dispersive, with higher frequencies traveling faster than lower frequencies.

Q and complex velocity

Since simple mechanical systems, composed of springs and dashpots and simple electric circuits also obey linear equations of the form of eqs. (2a,b), there are analogies between the quantities describing these systems and quantities in the stress-strain relation. For example, strain behaves like voltage, stress like current, and the complex compliance $\widehat{J}$ like the complex impedance of an electric circuit. Similar to the resonance phenomenon in circuits and mechanical systems, a Q can be defined by the average energy W per cycle divided by the energy lost or work done per cycle, ΔW:

$$Q=\frac{W}{\Delta W} \qquad (4)$$

Large Q's imply small energy loss; small Q's imply large loss. Q is a measure of the area contained in the hysteresis loop of a stress-strain cycle. The inverse of (4), Q^{-1}, is sometimes simply termed the *attenuation*.

Plane waves of frequency ω and propagating in the + x –direction can be defined by the phasor $\exp(i\omega t-\widehat{k}t)$ where $\widehat{k}$ is a complex wave number $\frac{\omega}{\widehat{c}}$ and $\widehat{c}$ is a complex velocity defined from the local density ρ and complex modulus $\hat{G}$, with

$$\widehat{c}=\sqrt{\frac{\widehat{G}}{\rho}} \qquad (5)$$

From the average energy density and loss per cycle of a complex plane wave it can be shown that $Q=\frac{\mathrm{Re}(\widehat{G})}{\mathrm{Im}(\widehat{G})}$. It is often less confusing to report the reciprocal parameter Q^{-1}, which represents the usually small perturbations to perfect elasticity.

The $Q^{-1}(\omega)$ relaxation spectrum

Since $\widehat{G}$ depends on frequency, Q also depends on frequency. Zener (1960) described the frequency-dependent effects on an elastic modulus of a solid having a single characteristic time τ for the relaxation of stress. A distribution of relaxation times can be constructed to give a Q^{-1} having a general dependence on frequency. The function $Q^{-1}(\omega)$ is called the *relaxation spectrum*. In the Earth and in many solid materials, the relaxation spectrum is observed to be slowly varying and nearly constant over a broad band of frequencies. A theoretical requirement is that the attenuation Q^{-1} cannot increase faster than ω^1 or decrease faster than ω^{-1}. Figure 2 shows how a continuous distribution relaxations can produce a Q^{-1} that is nearly constant with a frequency over a broad band. Once the limits of an absorption band are specified, however, it is not possible to have an arbitrarily high Q^{-1} (low viscoelastic Q) over an arbitrarily broad frequency band without making an unphysical large modulus defect ΔG.

Velocity dispersion

Although the dispersion in elastic moduli had long been known and predicted from the theories of viscoelasticity, it was only widely recognized in seismology when velocity models determined in the low-frequency band from the normal modes of the earth (0.0001 to 0.01 Hz) where compared with velocity models determined in a high frequency band (0.1 to 10 Hz) from body waves (Dziewonski and Anderson, 1981). The models were found to differ and the difference was found to agree with the amount of dispersion predicted from average Q models of the Earth. For example, since the preliminary reference Earth model (PREM), was derived from observations of both the travel times body waves as well as the eigenfrequencies free oscillations, it reports velocities referenced at both 0.001 Hz and at 1 Hz.

Another more subtle effect of this velocity dispersion can be seen in the propagation of pulses as body waves. A stress disturbance that propagates from its point of initiation as a symmetric narrow Gaussian or triangle-shaped function in time gradually evolves into an asymmetric pulse (Figure 3). High frequencies, traveling faster than low frequencies, are preferentially loaded into the front of the pulse (Futterman, 1962; Carpenter, 1967). Common theories for the physical mechanism of earthquakes as either frictional slip on a plane or a propagating crack triggered by tectonic stress often predict a far-field displacement pulse that has either a different or opposite form of asymmetry than that predicted for the effect of viscoelastic attenuation. These differences can assist in separating the effects of the source-time history from the effects of viscoelastic attenuation.

Effects of scattering

Equivalent medium

At frequencies that are so low that wavelengths are much larger than the characteristic scales of heterogeneity, the attenuative effects of scattering can usually be neglected. At sufficiently low frequency, little energy is lost to scattering, and the medium behaves like an equivalent medium, having properties that are an average of small-scale heterogeneities.

Stochastic dispersion

The most complicated domain in which to perform calculations is where the wavelength is on the order of the scale length of the heterogeneity (Figure 4). In this domain, the presence of heterogeneities can profoundly alter the propagation of the wavefield, both the initial cycle of a body wave pulse as well as the motion immediately following the initial cycle or *coda*. The effects of scattering can be calculated in a one-dimensional medium consisting of thin planar layers in which the velocity in each layer is assigned randomly (O'Doherty and Anstey, 1971; Richards and Menke, 1983). A prediction of such experiments is that body waves will exhibit a stochastic dispersion in which high-frequency energy is transferred into the coda following the first several cycles. This stochastic dispersion may have some biasing effects on measures of intrinsic attenuation. In measures of the spectrum taken over a narrow time window, different results can be obtained, depending on the length of window analyzed, with less attenuation of higher frequencies estimated from longer time windows.

Pulse measurements such as width and rise time may also be biased because higher-frequency energy has been transferred out of the pulse into the later coda. This behavior is opposite to the effects of intrinsic attenuation on a propagating pulse, in which higher-frequencies arrive at the beginning of the pulse. A symmetrically shaped displacement source pulse loses less of its symmetry as it propagates through the heterogeneous medium (Figure 5). Anisotropy of the scale lengths of heterogeneity can also be important factor (Hong and Wu, 2005), attenuation being strongest for paths for which the wavelength is on the order of the characteristic scale length in the medium in that direction.

Effects of anisotropy

The existence of general anisotropy in the real part of the elastic modulus has the potential to bias some estimates of anelastic attenuation from either shear wave pulses or surface waves. In a medium having general anisotropy, the decompositions of shear wave motion into SH and SV motion will each contain the interference of two orthogonal shear wave polarizations that are neither SH or SV (see *Shear wave splitting*). The broadening of the SH component due to the interference of two quasi-S waves arriving close in time can be mistaken for the broadening due to anelastic attenuation. The regions of the deep Earth characterized by the strongest elastic anisotropy are the upper 400 km of the mantle (Silver, 1996) and the lowermost 400 km of the mantle near the core-mantle boundary (Panning and Romanowiz, 2006). The effects of elastic anisotropy must be removed by combined analysis of SV and SH components of motion, resolving the polarizations of two quasi-S waves, before viscoelastic attenuation can be properly meaured.

Measurement and Modeling Attenuation

Measurements of amplitude of seismic waves may be taken directly from seismograms or from their frequency spectra. To measure the attenuation, we must predict its effects from a model and vary the parameters of the model to fit the observed amplitude, amplitude ratio, or waveform. The effects of intrinsic attenuation in any modeling algorithm operating in the frequency domain can be simply obtained by allowing elastic moduli and/propagation velocities to become complex. Elastic boundary conditions, reflection and transmission at boundaries, travel times, and amplitudes are calculated exactly as in a non-attenuating solid but with elastic moduli and associated velocities analytically continued to complex values. This step of analytic continuation of real moduli to complex moduli is the same whether one wishes to predict the waveform of a body wave or surface wave or spectrum of free oscillations. The size of the imaginary part of the elastic moduli, parameterized by the value of Q as a function of depth and frequency, is chosen to match an observed waveform, spectrum, amplitude ratio, or spectral ratio.

The attenuation operator for body waves

As an example of these procedures, consider an experiment with body waves. The effects on a body wave of source radiation, geometric spreading, reflection-transmission, and intrinsic attenuation are most conveniently expressed in the frequency domain by a product of complex functions. The complex $\widehat{\Omega}(\vec{x},\omega)$ spectrum of a body wave propagation from a point $\vec{x}_o$ to a receiver at $\vec{x}$ is

$$\widehat{\Omega}(\vec{x},\omega) = \vec{B}(\vec{x}_o,\vec{x},\omega)\ \widehat{S}(\omega)\ \widehat{A}(\omega) \qquad (6)$$

The function $\widehat{S}(\omega)$ is the Fourier transform of the source-time function. $\widehat{B}(\vec{x}_o,\vec{x},\omega)$ incorporates a product of reflection-transmission coefficients, reverberations at source and receiver, geometric spreading, and source radiation pattern. $\widehat{A}(\omega)$ is defined by

$$\widehat{A}(\omega) = \exp[i\omega \widehat{T}(\omega)] \qquad (7),$$

where $\widehat{T}(\omega)$ is the complex travel time obtained by integrating the reciprocal of complex velocity along a ray or normal to the wavefront of the body wave:

$$\widehat{T}(\omega) = \int_{ray} \widehat{c}(\omega)\, ds \qquad (8)$$

For body waves, the dominant effect of attenuation on amplitude and phase is given by $\widehat{A}(\omega)$. The effects of attenuation on reflection-transmission coefficients and geometric spreading, which have been lumped into $\widehat{B}$ are much smaller and can be neglected unless the attenuation is very large (Q is very small). For Q>> 1, $\widehat{A}(\omega)$ can be rewritten as

$$\widehat{A}(\omega) = \exp\left[\frac{-\omega\, t^*(\omega)}{2}\right]\ \exp\left\{i\omega\left[\mathrm{Re}\,\widehat{T}(\infty) - \frac{H[t^*(\omega)]}{2}\right]\right\} \qquad (9),$$

where

$$t^*(\omega) = \int_{ray} \frac{Q^{-1}}{\widehat{c}(\omega)}\, ds \qquad (10).$$

In eq. (9) attenuation effect is contained in the factor $\exp\left[\frac{-\omega t^*(\omega)}{2}\right]$, and the dispersive effect is in the factor $\exp\left\{i\omega\left[\mathrm{Re}\,\widehat{T}(\infty) - \frac{H[t^*(\omega)]}{2}\right]\right\}$. The operator H is a Hilbert transform. In a band of frequencies in which Q and t* are nearly constant

$$H[t^*(\omega)]/2 = \frac{\ln(\omega/\omega_0)}{\pi}\, t^* \qquad (11),$$

where ω_0 is a reference frequency contained in the band (Liu et al, 1976). The value of $T(\infty)$ need not be known and can be replaced by some reference time or predicted from an Earth model for the phase being analyzed. The Hilbert transform relation in eq. (11) for the dispersive phase of $\widehat{A}(\omega)$ says that $\widehat{A}(\omega)$ must be a minimum phase filter in the frequency domain. In general, the Fourier transform of the source-time function, $\widehat{S}(\omega)$, is not a minimum phase filter, which can be aid in the separation and discrimination of the source spectrum from the effects of $\widehat{A}(\omega)$ in the total expression for the far-field spectrum $\widehat{\Omega}(\vec{x},\omega)$.

The phase given by eq.(11) will be accurate only between and far from the low and high frequency corners of the relaxation spectrum. Accurate representations of $\widehat{A}(\omega)$ across a broad frequency band can be obtained for a general relaxation spectra by substituting expressions for complex velocity $\widehat{c}(\omega)$ in eq. (8) obtained by superposing multiple Zener relaxations centered on single relaxation times whose strength is varied to achieve a desired shape for the relaxation spectrum. A useful expression for $\widehat{c}(\omega)$ that is accurate for all frequencies across a relaxation spectrum, which is flat between two corner frequencies, can be derived from formulae for complex modulus given by Minster (1978), and is

$$\widehat{c}(\omega) = c_{ref}(\omega_0)\frac{\sqrt{1 + 2\pi Q^{-1}\ln[\psi(\omega)]}}{\mathrm{Re}\sqrt{1 + 2\pi Q^{-1}\ln[\psi(\omega_0)]}} \qquad (12a),$$

where

$$\psi(\omega) = \frac{i\omega + 1/\tau_1}{i\omega + 1/\tau_2} \qquad (12b).$$

with τ_1 and τ_2 the relaxation times corresponding to the low and high frequency corners respectively. $c_{ref}(\omega_0)$ is a real velocity at the reference frequency ω_0.

Most measurements of attenuation attempt to measure only the amplitude effect of attenuation through the term $\exp[-\omega t^*(\omega)/2]$ from the spectral shape of body waves. There are basically two types of experiments commonly reported: matching of (1) spectral decay rates and (2) spectral ratios. In experiment (1) a shape for the displacement source spectrum $\widehat{S}(\omega)$ is assumed usually to be a flat level followed by a decay of ω^{-2} above a corner frequency. The additional decay observed at high frequencies in data spectra is taken as a measure of t^*in $\exp[-\omega t^*(\omega)/2]$. In experiment (2) a ratio of two different seismic phases from the same source is observed in which the source spectrum is assumed to approximately cancel and the factor related to ratios of geometric spreading and near source and receiver crustal reverberations can be assumed to contribute a simple constant scalar factor. If the phases analyzed are recorded at the same receiver and are incident at nearly the same angles, then crustal reverberations at the source and receiver will approximately cancel. Both types of experiments usually apply some type of smoothing to the spectra to remove biasing effects of spectral holes caused by interfering crustal multiples, source complexities, scattering, and multipathing that are not included in the simple propagation model. Figure 6 illustrates an attenuation experiment of this type.

Since t* measures only the path-integrated effect of attenuation, many such experiments for different ray paths, bottoming at a range of different depths, are needed to construct a model of Q as a function of depth. Serious breakdowns in this approach, however, exist for cases in which the factorization of the observed spectrum into a product of a geometric spreading, source spectrum, and crustal effects is no longer accurate. One such case is when the body waves in question experience frequency dependent effects of diffraction near caustics or grazing incidence to discontinuities. The spectral ratio of PKnKP waves, for example, are dominated by the effects of frequency dependent reflection and transmission coefficients at grazing incidence to the core mantle boundary. Instead of decreasing linearly with increasing frequency, the observed spectral ratio increases with frequency and exhibits a curvature in a log-log plot, which is consistent with a Q near infinity ($Q^{-1}= 0$) in the other core (Cormier and Richards, 1976).

It is becoming more common to model and invert for viscoelastic attenuation parameters in the time domain, including not only the magnitude of the viscoelastic attenuation parameter Q^{-1}, but also its frequency dependence. Examples of such a study are the inversions for Q^{-1} in the inner core assuming either a viscoleastic (Li and Cormier, 2002) or a scattering origin of attenuation (Cormier and Li, 2002). In these studies the combined effects of mantle attenuation and source-time function were first modeled by fitting P waves observed in the great circle range 30^0-90^o. Attenuation in the liquid outer core was assumed to be zero. Parameters defining a viscoelastic relaxation spectrum in the inner core were then varied to match the observed PKIKP waveforms. Care must be taken to examine a broad range of attenuation parameters because waveform inversions of this type are very non-linear.

Free oscillations and surface waves

Measurements of attenuation in the low-frequency band of the free oscillations of the Earth are conducted in the frequency domain by observing the width of the individual resonance peaks associated with each mode. These measurements face special problems associated with the broadening produced by lateral heterogeneity of elastic Earth structure. This heterogeneity splits the degenerate modes of a radially symmetric Earth, making a set of modes that would have the same frequency have slightly different frequencies. The slightly different frequencies of the split modes may not be easily resolved in the data spectra and can be confused with the broadening of a single resonance peak of a mode caused by attenuation.

Lateral heterogeneity also complicates the measurement of viscoelastic attenuation of surface waves. Heterogeneity introduces focusing, defocusing and multipathing, all of which must be accurately modeled to understand the separate attenuative effects of viscoelasticity.

The frequency band of free-oscillation and surface waves (0.001 to 0.1 Hz), however, offers the best hope of obtaining radially symmetric whole-Earth models of viscoelastic attenuation in this frequency band. This is because lateral variations in attenuation structure are averaged by the gravest modes of oscillation and surface waves that make multiple circuits around the Earth. Computational advances have made the division between free-oscillation and surface wave studies fuzzier, with common approaches now amounting to time-domain modeling of complete low frequency (<0.1 Hz) seismograms for combined three-dimensional models of viscoelasticity and heterogeneity.

Numerical modeling

Fully numerical modeling of the seismic wavefield allows the combined effects of heterogeneity and viscoelasticity in three-dimensions to be predicted. If the numerical technique is formulated in the frequency domain, substituting a complex velocity for an assumed relaxation spectrum can incorporate viscoelastic attenuation.

If the technique is formulated in the time domain by a finite difference approach, it is neither simple or efficient to incorporate attenuation by convolution of the wavefield calculated in a non-attenuating medium with an attenuation operator $A(t)$ for individual waves propagating in the attenuating medium, where $A(t)$ is the Fourier transform of $\widehat{A}(\omega)$ defined in eq. (9). Instead, time-domain *memory functions* can be defined to describe a viscoelastic relaxation (Robertsson et al., 1994; Blanch et al., 1995) that can be integrated over time simultaneously with the equations describing particle velocity or displacement and stress. In practice, only three-memory functions, distributed evenly over the logarithm of their characteristic times, are required to simulate a broad frequency band in which Q^{-1} varies slowly.

Interpretation of attenuation measurements in the Earth

Shear versus bulk attenuation

In the most general theory of viscoleasticity, it is possible to have with energy loss to occur during both a cycle of volumetric strain as well as shear strain. Since the velocity of a P wave depends on both the bulk and shear moduli, the attenuation Q_P^{-1} of a P wave can be written as a linear combination of the attenuations Q_K^{-1} and Q_S^{-1} defined from complex shear and bulk moduli:

$$Q_P^{-1} = L\,Q_S^{-1} + (1-L)\,Q_K^{-1} \qquad (13),$$

where $(4/3)(V_S/V_P)^2$ and V_P and V_S are the compressional and shear velocities respectively (Anderson, 1989). Although plausible mechanisms for defects in bulk moduli have been found in both laboratory measurements and analytic models of specific attenuation mechanisms, measurements on real data find that bulk dissipation in the earth is small and, in most cases, can be neglected. One exception may occur when the pressure and temperature state in a narrow depth regions of the earth are close those near a phase transition, either solid-liquid or solid-solid. Except for these regions, intrinsic attenuation occurs almost entirely in shear, associated with lateral movement of lattice defects, grain boundaries and/or fluids rather than with changes in material volume. Hence, for viscoelastic attenuation purely in shear in Poisson solid, for which $V_P = \sqrt{3} V_S$,

$$Q_P^{-1} = \frac{4}{9} Q_s^{-1} \qquad (14),$$

and the parameter for path-integrated attenuation of S waves or t^*_S is approximately $4t^*_P$. Most experiments confirm these values. There is a suggestion, however, that the apparent Q_P^{-1} tends to approach Q_S^{-1} and $t^*_S < 4t^*_P$ at frequencies higher than 1 Hz. These observations are like evidence of scattering rather than of bulk attenuation because the effects of scattering increase at higher frequencies. With scattering, the apparent Q_S^{-1} tends to approach the apparent Q_P^{-1} especially when they are measured from pulse widths or spectra taken in a frequency band and medium for which wavelengths are on the order of richest heterogeneity scale lengths of the medium. Thus, the assumption of viscoelastic attenuation occurring mainly in shear can aid in separating the effects of scattering from intrinsic attenuation in body wave pulses.

Frequency dependence

When the results of attenuation measurements determined from free oscillations and body waves in the 0.0001 – 0.1 Hz band began to be compared with observations of body wave spectra in the 1-10 Hz band, it became apparent that even under the assumption of a white source spectrum that an increase in Q with frequency was necessary to explain the amplitude of spectra in the 1 –10 Hz band.

Thermal activation

Frequency dependence of viscoleastic attenuation has been interpreted in terms of physical mechanisms of attenuation that are thermally activated. In these mechanisms, the low frequency corner f_L is tied to a relaxation time τ_L, where $f_L = 1/(2\pi\tau_L)$. The time τ_L depends on temperature T and pressure P as follows:

$$\tau_L = \tau_0 \exp\left(\frac{E^* + PV^*}{RT}\right) \qquad (15),$$

where E* and V* are the activation energy and volume respectively. Both the low and high frequency corners (f_L, f_H) of an absorption band are assumed to be similarly affected, temperature and pressure acting to slide the absorption band through a band of frequencies. A typical width to expect for the relaxation spectrum of the mantle is about 5 orders of magnitude in frequency, $\tau_L / \tau_H = 10^5$ (Minster and Anderson, 1981; Anderson and Given, 1982). A simplified model of an absorption band with depth in the earth's mantle is shown in Figure 7. The movement of the absorption band toward lower frequencies (longer periods in the mantle below 400 km depth is consistent with the type of behavior show in Figure 8 for the t^*_S measured from shear waves of an earthquake. The difference in the location of the absorption band with respect to the band of seismic frequencies is consistent with models of the temperature and pressure profiles of the Earth's mantle for specific values of E* and V*. Relaxation times are also affected by the grain size of minerals, which may increase from mm to cm in the upper 400 km of the mantle (Faul and Jackson, 2005). A rapid increase in temperature with depth can rapidly change the location of the absorption band with respect to the seismic band. Given a specific temperature profile, estimated values of the activation energy and volume, and grain size, a combined shear velocity and Q_S profile can be predicted and modified to fit an observed shear velocity profile.

Regional variations

Romanowicz and Mitchell (2007) review and interpret both global and many regional variations in intrinsic attenuation, including correlations with velocity perturbations. Tomographic images of perturbations to seismic velocities and attenuations in the mantle can qualitatively be interpreted as images of lateral temperature variations, leaving open the possibility of additional contributions to the observed heterogeneity from chemical variations. In the upper mantle, tectonically active regions overlain by radiogenically younger crust are more attenuating than the mantle underlying inactive regions such as continental shields (Figure 9). The shape of the frequency dependence across the seismic band seems to remain similar in different regions, although the Q at a given frequency is lower for a tectonically young region than for an older shield region.

Generally, perturbations in attenuation Q^{-1} inversely correlate with those in shear wave velocity (Roth et al., 2000). The correlations between shear velocity and shear attenuation appear to be consistent with thermal activation, in which the dispersive effect of attenuation acts jointly with variations in the high-frequency corner of the mantle relaxation spectrum to produce the observed variations in travel time and frequency content. Deep chemical differences between the upper mantle beneath shields and that beneath young continents and oceans as well as in the deep mantle, however, have been suggested by comparing anomalies in shear velocity versus bulk velocity V_K , where $V_K = \sqrt{V_P^2 - (4/3)V_S^2}$. Milder lateral temperature differences in the mid- and lower mantle tend to make the relaxation spectrum more laterally stable in height, width and location within a frequency band, reducing the observed lateral heterogeneity in velocity and attenuation in these regions.

Global models of attenuation (e.g., Gung and Romanowicz, 2004) often do not have the resolving power to detect spatially concentrated regions of high attenuation and sharp spatial gradients found in regional studies beneath and near island arcs, mid-ocean spreading ridges, and hot mantle plumes. The dense path coverage required of higher frequency (0.1 to 2 Hz) body waves needed to resolve smaller spatial scales usually is lacking except in regions containing dense seismic networks. Even larger scale, long established lateral variations, such as high attenuation west of the Rocky Mountains in North America and low attenuation east (Der et al., 1982), are not very apparent in some global studies (Warren and Shearer, 2002).

Strain dependence.

Laboratory measurements of Q in rocks find dependence in strain beginning at strains of about 10^{-6}. The strain dependence decreases with confining pressure. The Q is also strongly dependent on moisture and interstitial fluids between cracks in rocks and grain boundaries and soils. These observations are consistent with a physical mechanism of frictional sliding of cracks and cracks. Unlike viscoelastic relaxations, which are representative of all linear mechanisms, frictional sliding is an inherently nonlinear mechanism, depending on strain amplitude.

Estimates where nonlinear effects occur in particular data may be made by calculating the strain associated with the seismic wave being analyzed. A rough estimate can be obtained by assuming that the wavefront is a plane wave and dividing the particle velocity by the propagation velocity. For example, the particle velocity of body waves observed in strong ground motion recordings from 0 km to 10 km from the hypocenter of a magnitude 6 earthquake are typically 0.01m/sec. If the body wave propagates at 3 km/sec, the strain observed at the strong ground motion site is roughly 0.01/ms/ec divided by 3×10^3 m/sec or epsilon = 3.3×10^{-5}. This value is likely to be in the nonlinear regime of surficial rocks having open cracks or pores. In this strain regime it becomes important to solve the elastic equation of motion with non-linear terms in its rheology (Bonilla et al., 2005), including terms proportional to the square of strain.

Summary

The intrinsic attenuation of seismic waves in the earth has been found to be consistent with loss mechanisms that are thermally activated. The observed regional and frequency dependences of seismic Q agree with the expected lateral variations in a geotherm having a rapid temperature increase in the upper 400 km of the mantle, followed by a slower vertical and lateral variation in the mid- and lower mantle. High velocities correlate with regions of low attenuation; low seismic velocities correlate with regions of high attenuation. Measurements are consistent with losses primarily in shear rather than bulk deformations.

The existence of lateral heterogeneity in the elastic properties of the Earth complicates the measurement of viscoelastic properties. The longer scale lengths of heterogeneity can split modes of free oscillation and focus and defocus body waves and surface waves. Shorter scale lengths scatter seismic energy, broaden the waveforms of body waves, and redistribute energy into different time and angular windows. Observations that are useful for discriminating between the effects of scattering attenuation versus viscoelastic attenuation include the ratio of apparent P wave attenuation to apparent S wave attenuation, the rate of velocity dispersion within a frequency band, and the apparent viscoelastic modulus defect. The intensity of heterogeneity in percent fluctuation of velocities and densities is higher at shorter scale lengths at shallower depths in the Earth's crust and upper mantle. There is still a need for experiments that determine finer details of how the distribution of heterogeneity changes with depth and lateral location in the Earth and its anisotropy of scale lengths. Many, if not most experiments, have not completely removed the effects of heterogeneity on the apparent attenuation, making their results an upper bound on the viscoelastic Q^{-1}.

Laboratory experiments find a transition from linear to non-linear rheology at strains on the order of 10^{-6}. The observed strain dependence of Q and its dependence on pressure in the shallow crust agree with a mechanism of frictional sliding of cracks. It is still unknown how and at what strain levels linear superposition begins to break down close to a seismic source.

Although a consensus has been reached on the major features and thermal activation of intrinsic attenuation in most of the Earth's upper mantle, this is less true of other deep regions of the Earth. Definitive experiments are still needed for the distribution of Q in the lowermost 400 km of the mantle, where increased lateral heterogeneity exists across a broad spatial spectrum complicating the separation of its effects from those of viscoelasticity. A concept unifying lateral variations in velocity, elastic anisotropy, scattering, and apparent attenuation in the uppermost inner core is needed (e.g., Calvet and Margerin, 2008).

Vernon F. Cormier

Bibliography

Anderson, D.L., and Given, J.W., 1982. The absorption band Q model for the Earth. *J. Geophys. Res.* 87: 3893-3904.

Anderson, D.L., 1989. *Theory of the Earth*. Boston: Blackwell Scientific Publications.

Blanch, J.O., Robertsson, J.O.A., and Symes, W.W., 1995. Optimally efficient constant Q modeling. *Geophysics* 60: 176-184.

Boatwright, J., and Choy G., 1986. Teleseismic estimates of the energy radiated by shallow earthquakes, J. *Geophys. Res.* 91: 2095-2112.

Bonilla, L. F., Archuleta, R.J., and Lavallée, D., 2005. Hysteretic and dilatant behavior of cohesionless soils and their effects on nonlinear site response: field data, observations and modeling, *Bull. Seism. Soc. Am.* 95: 2373-2395.

Calvet, M., and Margerin, L., 2008. Constraints on grain size and stable iron phases in the uppermost inner core from multiple scattering modeling of seismic velocity and attenuation. *Earth Planet. Sci. Lett*. 267:, 200-212.

Carpenter, E.W, 1967. Teleseismic signal calculated for underground, underwater, and atmospheric explosions. *Geophysics* 32:17-32.

Choy, G.L., and Cormier, V.F., 1986. Direct measurement of the mantle attenuation operator from broadband P and S waves. *J. Geophys. Res.* 91: 7326-7342.

Choy, G.L., and Boatwright, J.L., 1995. Global patterns of radiated seismic energy and apparent stress. *J. Geophys. Res*. 100: 18,205-18,228.

Cormier, V.F., and Richards, P.G., 1976. Comments on "The Damping of Core Waves" by Anthony Qamar and Alfredo Eisenberg. *J. Geophys. Res.* 81: 3066-3068.

Cormier, V.F., and Li, X., 2002. Frequency dependent attenuation in the inner core: Part II. A scattering and fabric interpretation, *J. Geophys. Res*. 107(B12): doi: 10.1029/2002JB1796.

Dalton, C.A., Ekstrom, G., and Dziewonski, A.M., 2009. Global seismological shear velocity and attenuation: A comparison with experimental observations. Earth Planet. Sci. Lett. 284: 65-75.

Der, Z.A., McElfresh, T.W., and O'Donnell, 1982. An investigation of regional variations and frequency dependence of anelastic attenuation in the United States in the 0.5-4 Hz. band, *Geophys. J. Roy. Astron. Soc.* 69: 67-100.

Dziewonski, A.M., and Anderson, D.L., 1981. Preliminary reference Earth model. *Phys. Earth and Planet. Int*. 24-297-356.

Faul, U.H., Jackson, I., 2005. The seismological signature of temperature and grain size variations in the upper mantle. *Earth Planet. Sci. Lett.* 234: 119-134.

Futterman, W.I., 1962. Dispersive body waves. *J. Geophys. Res*. 67: 5279-5291.

Gross, B., 1953. *Mathematical Structure of the Theories of Viscoelasticity*, Paris: Hermann.

Gung, Y, and Romanowiz, B.A., 2004. Q tomography of the upper mantle using three component long period waveforms. *Geophys. J. Int.* 147: 831-830.

Hong, T-K., and Wu, R-S., 2005. Scattering of elastic waves in geometrically anisotropic random media and its implication to sounding of heterogeneity in the Earth's deep interior, Geophys. J. Int. 163: 324-338.

Jackson, I., 1993. Progress in the experimental study of seismic attenuation. *Ann. Rev. Earth Planet Sci*. 21: 375-406.

Jackson, I., Webb, S, Weston, L., and Boness, D., 2005. Frequency dependence of elastic wave speeds at high temperature: a direct experimental demonstration. *Phys. Earth Planet. Inter.,* 148:, 85-96.

Jackson, I., 2007. Properties of rocks and minerals – physical origin of anelasticity and attenuation in rocks. In: Schubert, G. (Ed.), *Treatise on Geophysics*, 2, Elsevier, 493-525.

Kaelin, B., and Johnson, L.R., 1998. Dynamic composite elastic medium theory. Part II. Three-dimensional media. *J. Appl. Phys* 84: (1998) 5458-5468.

Li, X, and Cormier, V.F., 2002. Frequency dependent attenuation in the inner core: Part I. A viscoelastic interpretation. *J. Geophys. Res*. 107(B12): doi: 10.1029/2002JB001795.

Liu, H-P., Anderson, D.L., and Kanamori, 1976. Velocity dispersion due to anelasticity: implications for seismology and mantle composition. *Geophys. J. R. Astr. Soc.*, 47:41-58.

Minster, J.B., 1978. Transient and impulse responses of a one-dimensional linearly attenuating medium — I. Analytical results. *Geophys. R. Astron. Soc*. 52*:* 479-501.

Minster, B. ,and Anderson, D.L., 1981. A model of dislocation-controlled rheology for the mantle, *Phil. Trans. R. Soc. Lond.* 299: 319-356.

Nowick, A.S., Berry, B.S., 1972. *Anelastic Relaxation in Crystalline Solids*. New York: Academic. 677pp.

O'Doherty, R. F. and Anstey, N. A., 1971. Reflections on amplitudes*. Geophys. Prosp.* 19: 430-458.

Panning, M.P., and Romanowicz, B.A., 2006. A three dimensional radially anisotropic model of shear velocity in the whole mantle. Geophys. J. Int. 167: 361-379.

Richards, P.G., and Menke, W., 1983. The apparent attenuation of a scattering medium. *Bull. Seism. Soc. Am.* 73: 1005-1021.

Robertsson, J.O.A., Blanch, J.O., and Symes, W.W., 1994. Viscoelastic finite-difference Modeling. *Geophysics* 59: 1444-1456.

Romanowicz, B., Mitchell, B., 2007. Deep Earth structure: Q of the Earth from crust to core. In: Schubert, G. (Ed.), *Treatise on Geophysics*, 1, Elsevier, 731-774.

Roth, E. G., Wiens, D.A., and Zhao, D., 2000. An empirical relationship betweeen seismic attenuation and velocity anomalies in the upper mantle. *Geophys. Res. Lett*., 27: 601-604.

Silver, P.G.,1996. Seismic anisotropy beneath the continents: Probing the depths of geology. *Ann. Rev. Earth Planet. Sci.* 24: 385-432.

Warren, L.M., and Shearer, P.M., 2000. Investigating the frequency dependence of mantle Q by stacking P and PP spectra. *J. Geophys. Res.,*105(B11): 25391-25402.

Warren, L.M., and Shearer, P.M. 2002. Mapping lateral variations in upper mantle attenuation by stacking P and PP spectra. J. Geophys. Res. 107 (B12): 2342, doi:10.1029/2001JB001195.

Zener, C., 1960. Elasticity and Anelasticity of Metals, Chicago: The University of Chicago Press.

Cross-references

Body waves
Earthquake tomography
Earthquake strong ground motion forecast
Elastic waves in homogeneous and inhomogeneous media
Elastic wave propagation: principles
Elastic properties of rocks
Energy partitioning of seismic waves
Free oscillations of the Earth
Lithosphere, mechanical Properties
Mantle D" Layer
Mantle rheology
Numerical methods: Finite difference
Seismic phase names, the IASPEI standard
Seismic monitoring of nuclear explosions
Seismic source, theory
Seismic anisotropy
Seismic, diffraction
Seismic, ray theory
Seismic, scattering
Seismic, velocity-temperature
Seismology, source modeling
Shear wave splitting
Structure of Earth's core
Structure of Earth's lower mantle
Thermal properties of rocks
Upper mantle structure

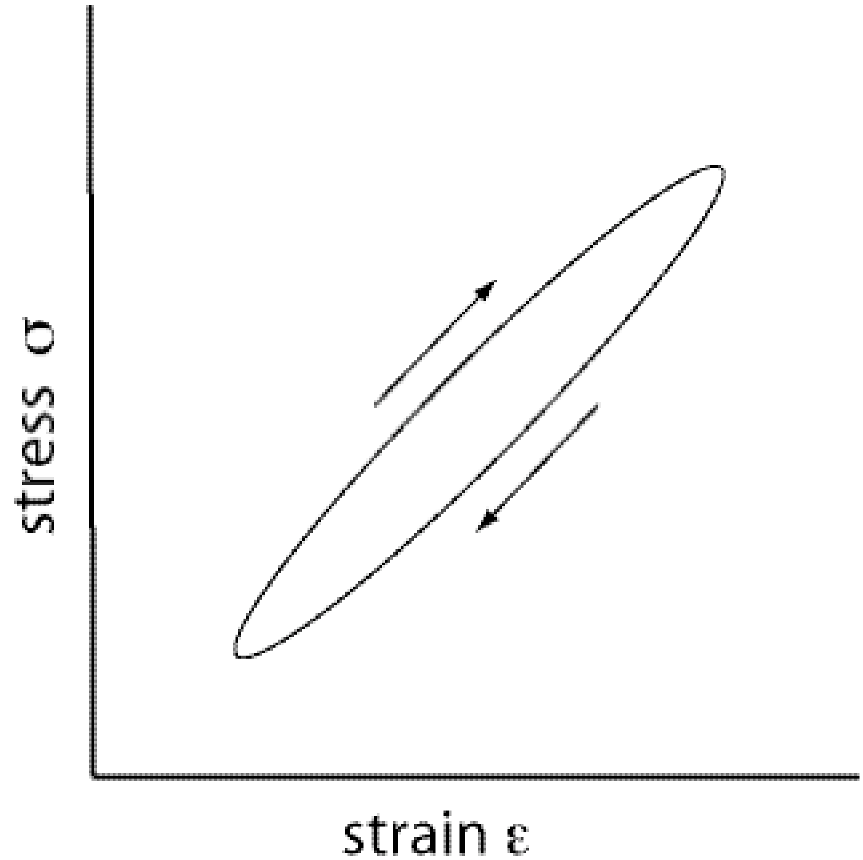

Figure 1 Stress-strain hysteresis curve showing the behavior of strain due a cycle of applied stress.

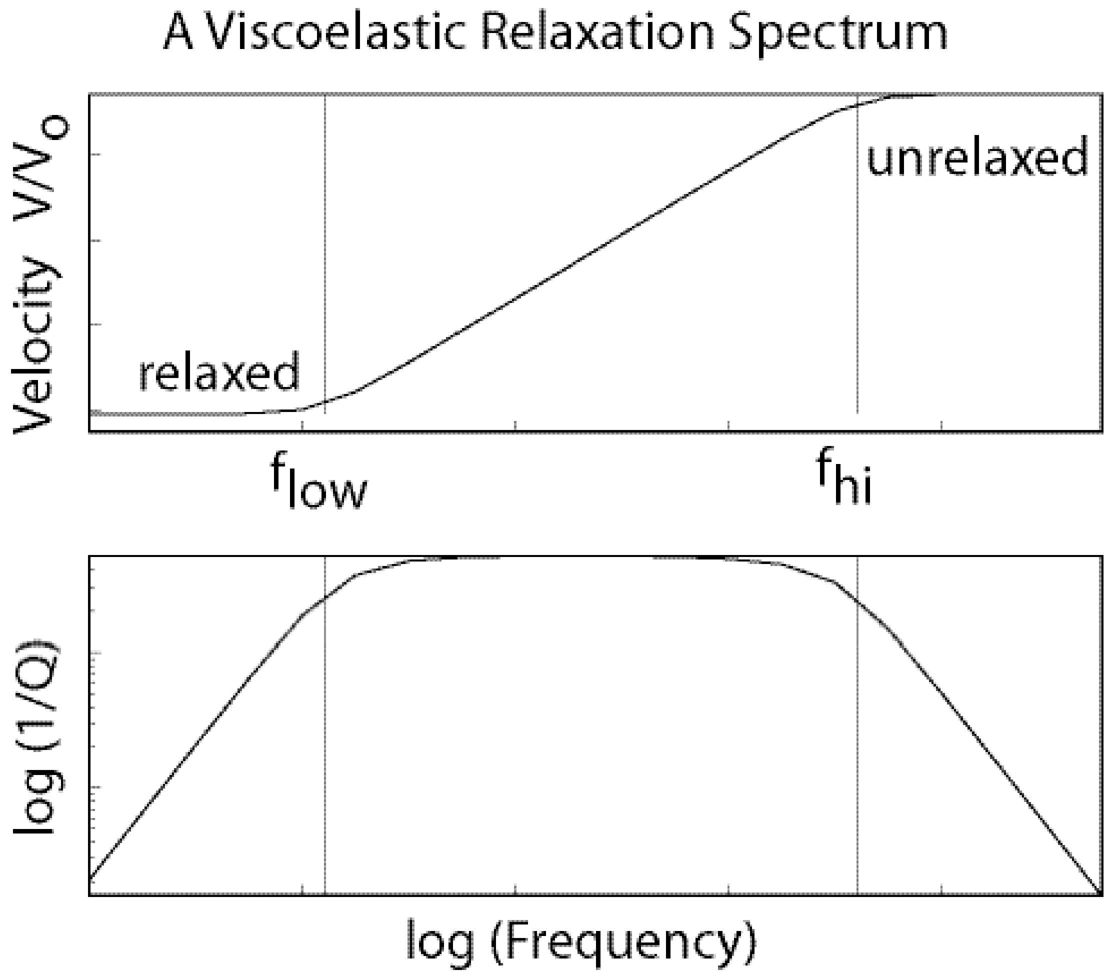

Figure 2 Viscoelastic dispersion of seismic velocity and attenuation showing a relaxation spectrum constant with frequency between two corner frequencies.

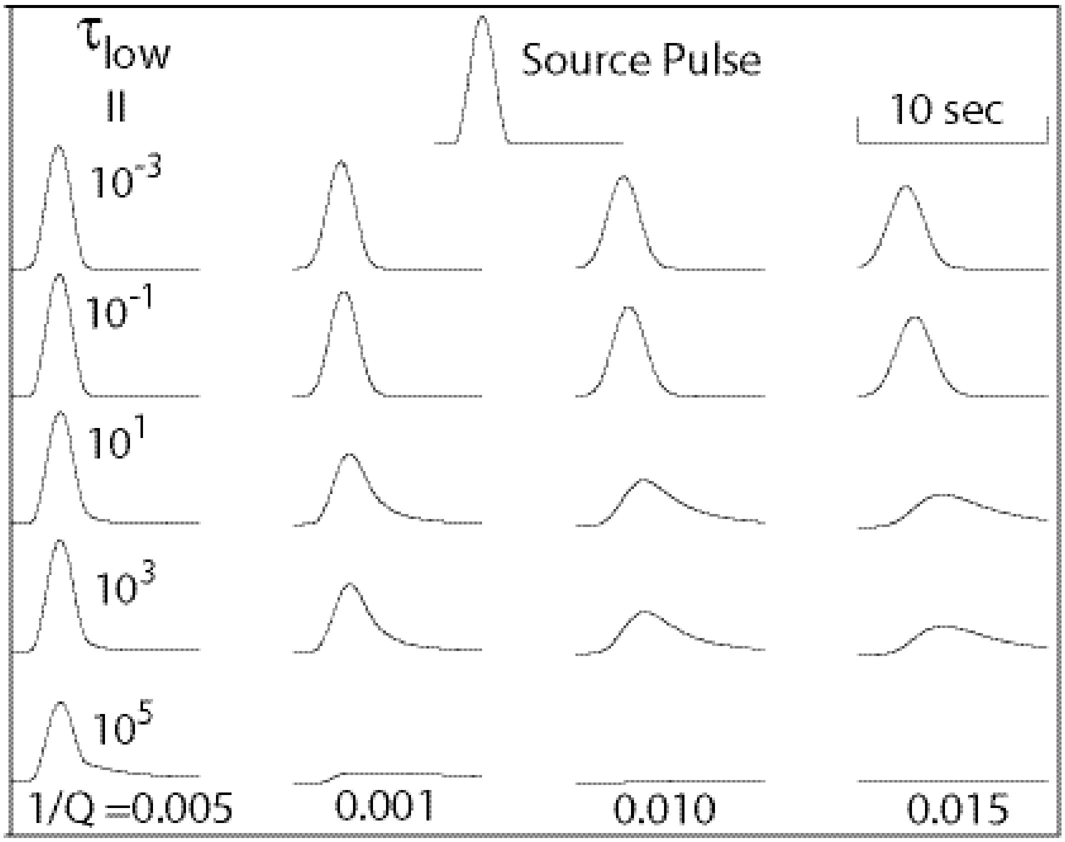

Figure 3 Pulse distortion showing the effects of viscoelastic dispersion for variable low frequency corner and peak attenuation.

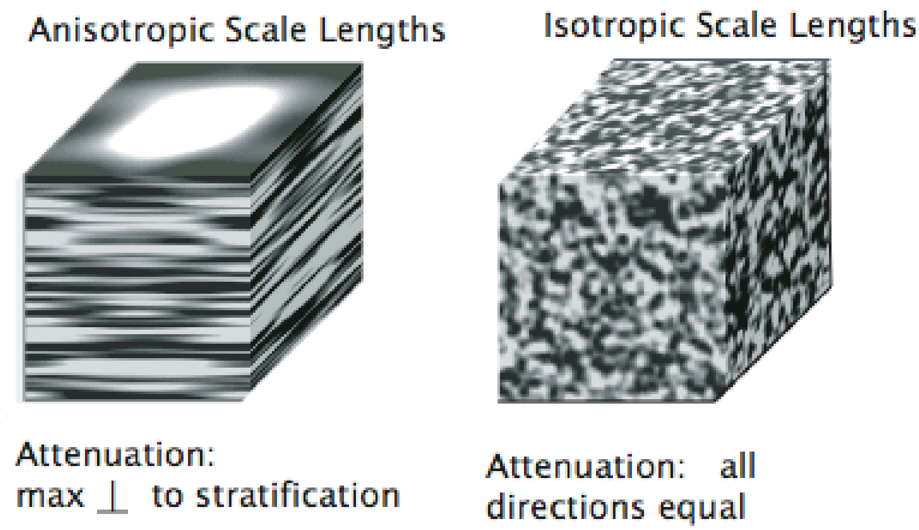

Figure 4 Example types of small-scale heterogeneity in the Earth and the directional dependance of attenuation due to forward scattering transferring high frequency from a body wave pulse to its coda.

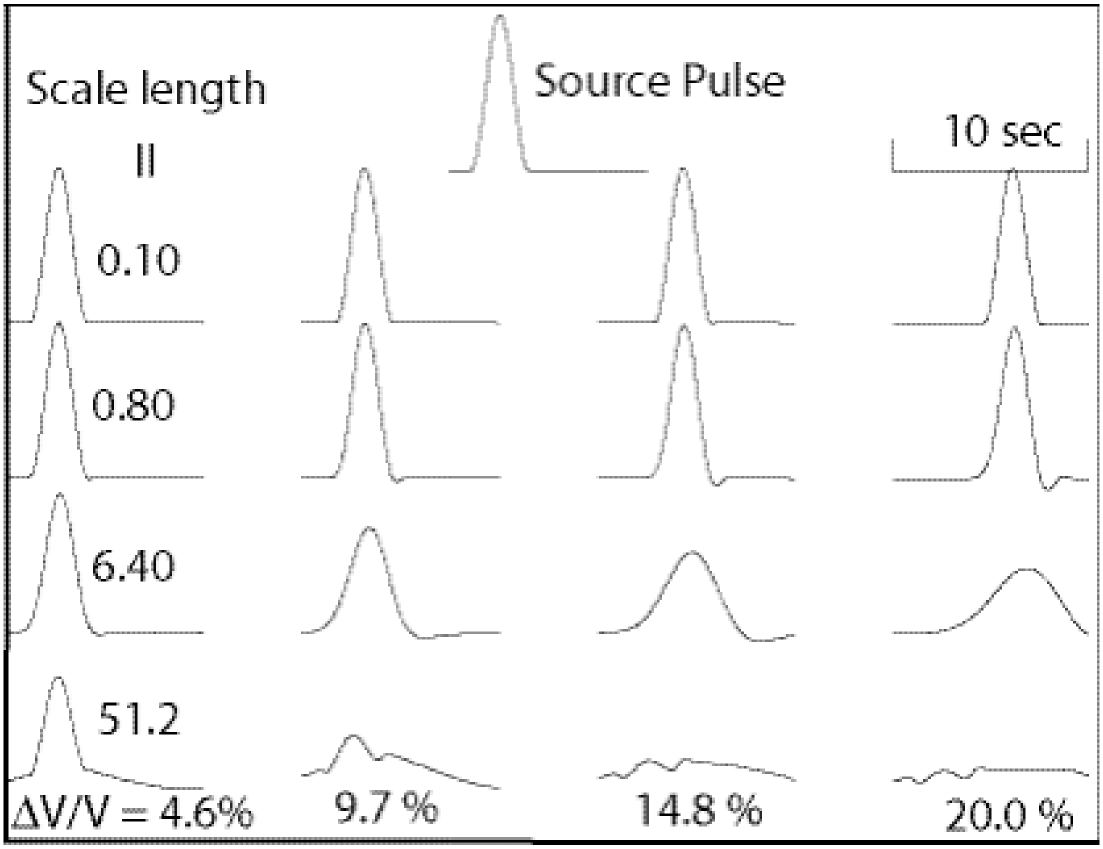

Figure 5 Pulse distortion showing the effects of scattering attenuation for variable scale lengths and velocity perturbation calculated by Cormier and Li (2002) using the Dynamic Composite Elastic Modulus (DYCEM) theory of Kaelin and Johnson (1998).

$$t^*_P = \frac{\ln(A_{PP}) - \ln(A_P)}{\pi f}$$

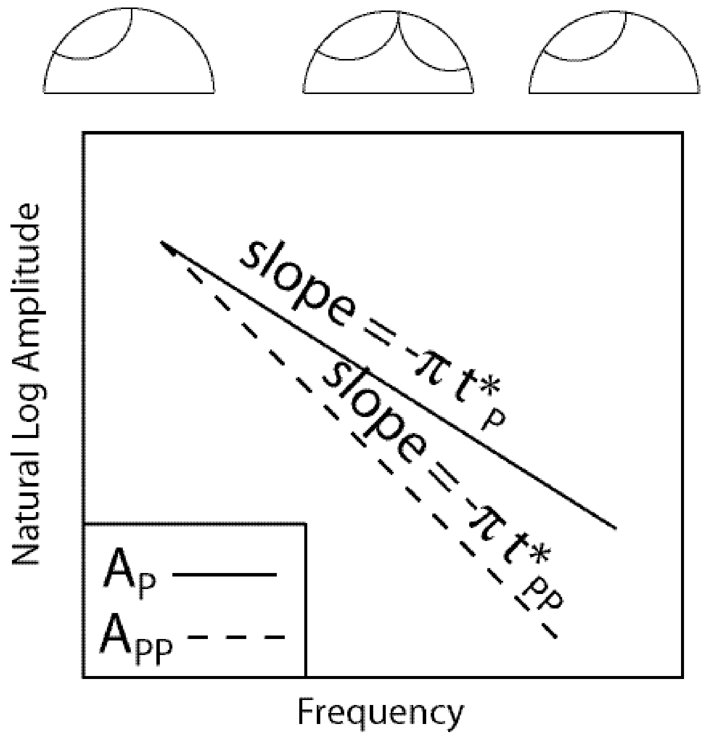

Figure 6 Measurement of the path integrated attenuation t* of P waves in the mantle from a log-log plot of stacked PP and P spectra above the corner frequency of magnitude 5.5 to 6 earthquakes; adapted from figures in Warren and Shearer (2000).

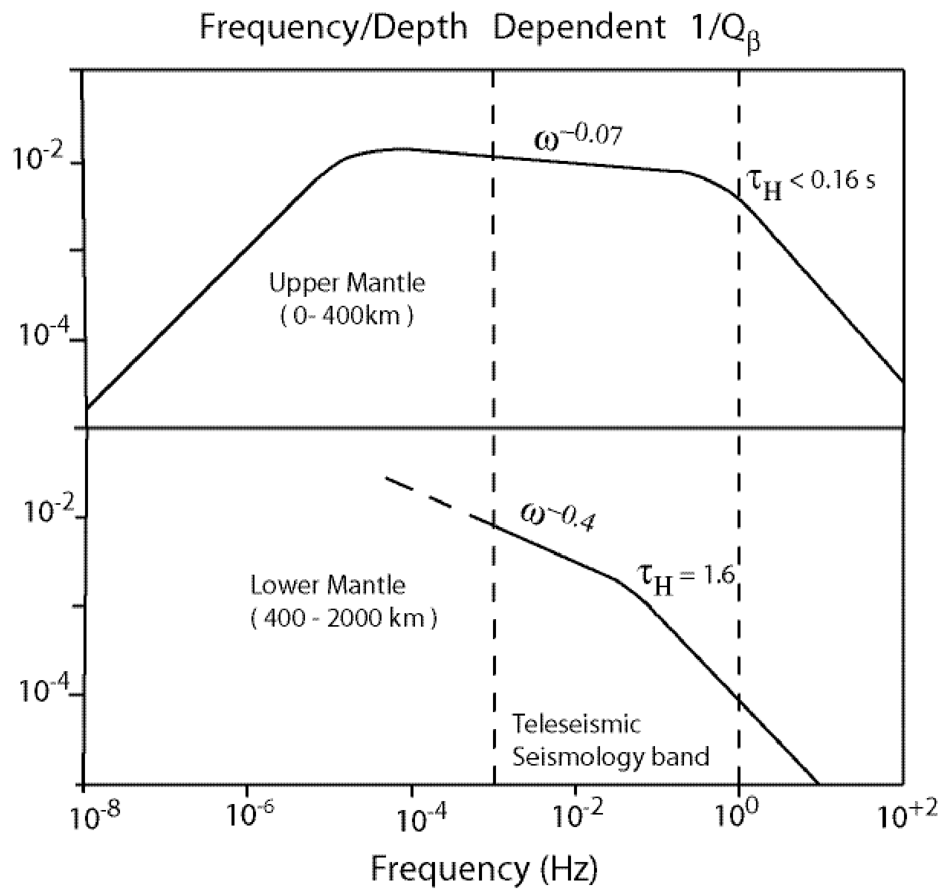

Figure 7 A frequency and depth dependent model of shear attenuation in the Earth's mantle derived from modeling broadband shear waves. This model has been used by the National Earthquake Information Center (NEIC) to correct for viscoelastic attenuation in the reported radiated elastic energy from earthquakes (Boatwright and Choy 1986; Choy and Boatwright, 1995).

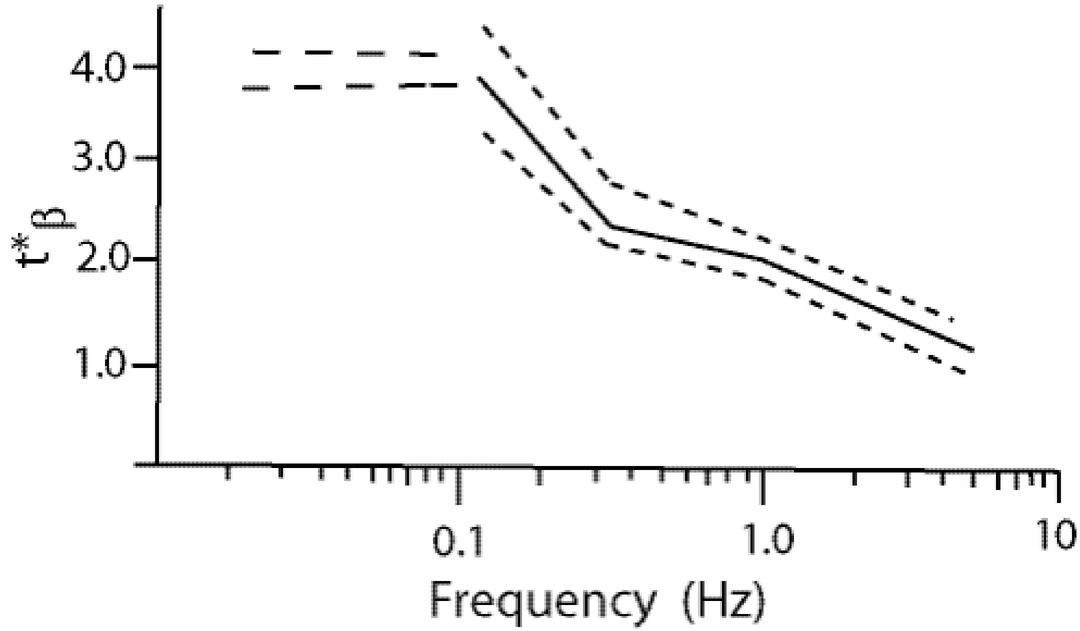

Figure 8 Path integrated attenuation t* of S waves in the mantle as a function of frequency determined from modeling broad band shear waves predicted from the frequency and depth-dependent attenuation model shown in Figure 7 (Choy and Cormier, 1986).

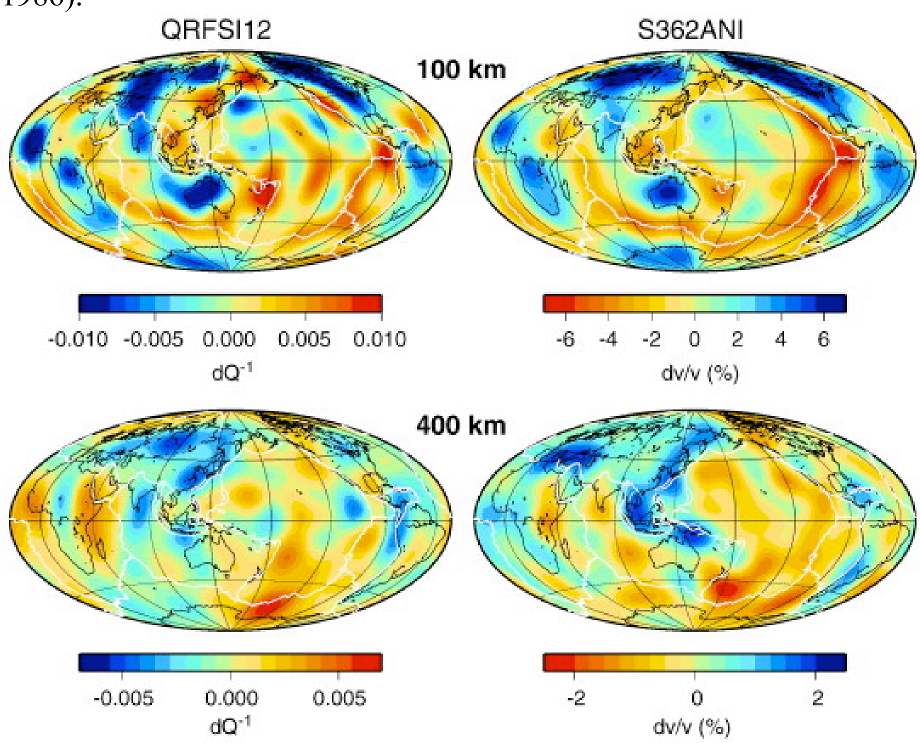

Figure 9 Inverted upper mantle shear velocity perturbations and shear attenuation from Dalton et al. (2009)